



THE EFFECT OF THE SOL-GEL PH ON THE PROPERTIES OF Al_2O_3 - AND SiO_2 -COATINGS ON LOW-ALLOYED 08kp STEEL

H. O. Kudryakova¹, E. P. Grishina^{1,2}, L. M. Ramenskaya¹

Kudryakova N.O., Candidate of Technical Sciences; Grishina E.P., Doctor of Technical Sciences, Associate Professor; Ramenskaya L.M., Candidate of Chemical Sciences, Associate Professor

¹Laboratory 1-8. Structure and dynamics of molecular and ion-molecular solutions of G.A. Krestov Institute of Solution Chemistry of the Russian Academy of Sciences, Akademicheskaya st., 1, Ivanovo, Russia, 153045

²Scientific Disciplines Department, Ivanovo Fire and Rescue Academy of the Russian Ministry for Emergency Situations, Stroiteley ave., 33, Ivanovo, Russia, 153040

E-mail: kno@isc-ras.ru, epg@isc-ras.ru, lmr@isc-ras.ru

Keywords:

sol-gel, oxide coating, corrosion protection coating, structural steel, aluminium oxide, silicon oxide, potentiometry, electrochemical impedance spectroscopy

The article concerns with the possibility and properties of thin-layer anticorrosive ceramic coatings on low-alloyed 08kp steel - two-layer oxide-aluminium, oxide-silicon and two-component Al_2O_3 - SiO_2 -coatings. In order to obtain the coatings by hydrolytic polycondensation of aluminium isopropoxide and tetraethoxysilane we prepared boehmite sols/gels with pH = 5 and 9 and hydrated silicon oxide with pH = 9 respectively. We made the mixtures of alumina gel and siliceous gel (pH = 9) in 1:4 and 4:1 ratios to obtain bicomponent coatings. These colloidal systems are characterised by pH-metry, particle size analysis and zeta-potential analysis. The morphology of the coatings includes the scanning electron microscopy. The results show that only the oxide-aluminium coatings have a homogeneous structure, while the SiO_2 - and Al_2O_3 - SiO_2 -coatings after heat treatment have defects in the form of micro-crack meshes. The assessment of protective properties of the coatings was in a 3.5% sodium chloride solution at $(23 \pm 1)^\circ\text{C}$ using electrochemical methods. Study contains the corrosion current densities calculations based on corrosion diagrams. Only single-component Al_2O_3 -films and two-component films with high aluminium oxide content have a protective effect. Electrochemical impedance spectroscopy data modeled the metal-film-electrolyte interface using an equivalent electrical circuit. The work contains the calculations of the values of the circuit parameters and their variation as a function of sample exposure time. The oxide-aluminium films made from aluminogel with pH = 5 and two-component Al_2O_3 - SiO_2 films of 4:1 composition show the best results.

Introduction

Low-alloy steel is a widely used and readily available construction material, but it does not have sufficient corrosion resistance, which limits its use without specialised corrosion treatment [1]. This treatment generally involves the application of coatings to prevent contact of metals with corrosive environments.

The one of the promising type of insulating coating are oxide (ceramic) coatings produced by sol-gel technology [2, 3]. The sol-gel technology has significant advantages [2-5]. It includes



the possibility of obtaining thin oxide films at temperatures close to room temperature, in contrast to traditional ceramic processing technologies, as well as the possibility to influence the chemical and technological processes and the final coating properties. The resulting oxide materials are structures ranging from sols in the form of nanoparticles to continuous polymer gels, depending on the rate of each of these reactions and the subsequent drying and processing stages. Also an advantage of the sol-gel coating technology is its eco-friendly nature.

Yoldas' [6-8] method of producing thin sol-gel films on various substrates is based on the controlled hydrolytic polycondensation of organic metal or silicon compounds with the participation of acid or alkali process speed regulators (catalysts/peptisators). The problem of ceramic dielectric films on the surface of iron alloys, aluminium and silicon oxides is the most relevant one. These coatings are highly chemically and thermally resistant and can form a physical barrier to the penetration of corrosive components to the metal surface. Thus they can improve metals corrosion characteristics. The anticorrosive Al_2O_3 -coatings on steels contribute to a significant shift of potential to the positive direction and a decrease of corrosion current, increase resistance to pitting corrosion [9-14]. Using of SiO_2 sol-gel coatings on steel was not very effective, although an improvement in corrosion performance was observed compared to untreated samples [15-18]. These results can be explained by the use of colloidal solutions with low pH values, to which iron-based alloys are sensitive, as well as to annealing, leading to cracking of the formed oxide layer. However, research in this area needs to be developed in order to find conditions for obtaining coatings with higher corrosion protection.

This paper presents the results of a study of the effect of acid and alkaline peptization of hydrolysates of organic compounds of aluminium and silicon on the properties of the corresponding hydrogels obtained by the Yoldas' method as well as on the anticorrosion properties of coatings formed on low-alloyed 08kp steel.

Experimental part

1. Materials and reagents

Oxide coatings were applied to 1×5 cm samples of 08kp carbon construction steel (strip, GOST 1577-93). Composition, %: Fe ~98, C 0.05-0.11, Si to 0.03, P to 0.035, As to 0.08, S to 0.04, Mn 0.25-0.5, Ni to 0.25, Cr 0.1-0.25. Samples without corrosion were previously degreased with acetone, then further in a solution of $\text{Na}_2\text{CO}_3 \cdot 10\text{H}_2\text{O}$ (40 g/l) + $\text{Na}_2\text{HPO}_4 \cdot 12\text{H}_2\text{O}$ (40 g/l) at 75–85 °C for 15 minutes, washed in hot, then in cold water, air dried at room temperature. The surface of the samples was activated by HNO_3 solution (1:1) treatment for 15 seconds.

Aluminum isopropoxide $\text{C}_9\text{H}_{21}\text{AlO}_3$ ($\text{Al}(\text{O}-i\text{-Pr})_3$, where $-i\text{-Pr} = (-\text{CH}(\text{CH}_3)_2$, produced by Acros organics, 98%, CAS №555-31-7), distilled water and tetraethoxysilane $\text{C}_8\text{H}_{20}\text{O}_4\text{Si}$ ($\text{Si}(\text{C}_2\text{H}_5\text{O})_4$, produced by ECOS - 1, h.p. were used to prepare hydrated aluminum and silicon oxide sols/gels respectively. Fig. 1. The structural formulae of compounds.

Peptization of the resulting sols provided by acetic acid (ch.p.) or by 10% ammonia (ch.p.).

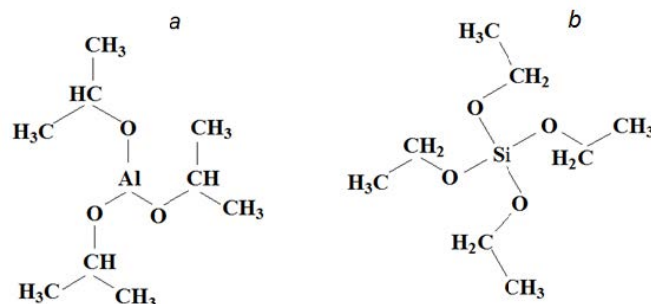
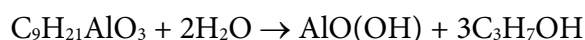


Fig. 1. Structural formulae of aluminium isopropoxide (a) and tetraethoxysilane (b)

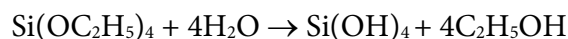
2. Preparation of sol-gel systems

Preparation of boehmite sols. Aluminium isopropoxide (AIPO) was dissolved in hot (85-90 °C) distilled water under continuous stirring. Molar ratio AIPO:H₂O = 1:100. Under these conditions, AIPO undergoes hydrolysis to form boehmite:



After completion of the formation of AlO(OH) at the same temperature, the boehmite hydrosol was peptised using acetic acid or ammonia solutions. During acidic peptization the molar ratio of the components of the reaction mixture AIPO:H₂O:acid, according to the Yoldas' procedure, was 1:100:0.15; during alkaline peptization the pH value was maintained at ~11. In both reactions we observed a lucidity of the colloidal solution after continuous stirring at the indicated temperature for ~2 hours. For 24 hours sol-gel transition occurred in the colloidal system. Characteristics of the prepared gels with acidic and alkaline peptidation are: pH equal to 5 and 9.5, average particle size of boehmite 300 and 100 nm respectively. The aluminium concentration in the obtained systems was 1.25 g/l.

Siliceous gel preparation. Siliceous gel was prepared by hydrolysis of tetraethoxysilane (TEOS) in a mixture of H₂O:C₂H₅ON (volume ratio 5:1) at a reactant ratio of TEOS:(H₂O/C₂H₅ON) = 1:100, at room temperature. Under these conditions, TEOS is hydrolysed by the reaction



Polycondensation reactions of the hydrolysis products take place along with the hydrolysis products take place along with the hydrolysis reactions of TEOS. The polycondensation process of siliceous gel was carried out in both acidic (acetic acid solution) and alkaline (ammonia solution) media at pH ~5 and ~9.5 respectively. The particle size of the siliceous gel is in the range 10-140 nm. The silicon concentration in the obtained systems was 1.25 g/l.

For all the colloids prepared, the sol-gel transition was accompanied by the formation of a translucent gel (Fig. 2).

Preparation of mixed AlO(OH)-Si(OH)₄ gels. In order to study the mutual influence of the gels on the properties of the coatings obtained, gels

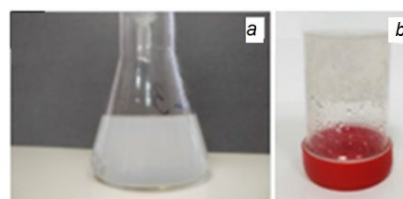


Fig. 2. Sol (a) and gel (b) produced using peptiser solutions



of the composition $\text{AlO}(\text{OH})\text{-Si}(\text{OH})_4$ ($\text{pH} = 9$) were prepared by direct mixing the components at their volume ratio of 1:4 and 4:1.

3. Coating application

We use both individual alumina gel and siliceous gel as well as their mixtures in the above mentioned volume ratios. A sample of 08kp steel with a pre-greased prepared dry surface was dipped into the gel, incubated for three minutes and then quickly removed. The samples were air dried (for alkaline gels) or dried in an air-ammonia atmosphere (for gels with $\text{pH} < 7$) at room temperature, then heat treated in an air atmosphere at $500\text{ }^\circ\text{C}$ for one hour.

The surface preparation of gels with $\text{pH} > 7$ included a surface activation stage in HNO_3 solution (1:1) for 15 seconds followed by rinsing the sample with cold water.

We applied the second layer on top of the fully formed first layer in full compliance with the procedure, except for the activation stage (for alkaline colloids).

4. Research methodology

We determine the physico-chemical characteristics of the prepared gels by Kellymeter pH-009(I) (Kelly Union Electronics, Hong Kong), Zetasizer Nano particle size and zeta-potential analyser (Malvern Instruments Ltd., UK).

The morphology of the coatings was studied by scanning electron microscopy (SEM, Vega 3 SBH scanning electron microscope, Tescan, Czech Republic).

Anticorrosive properties of coatings in 3.5% aqueous solution of NaCl at $(23 \pm 1)\text{ }^\circ\text{C}$ were studied by electrochemical methods of potentiometry-, voltammetry (reference electrode - saturated silver chloride, the loop electrode - Pt; PI 50-Pro-3 pulse potentiometer with automatic data logging and PS Pack2 software, Elins, Russia) and electrochemical impedance spectroscopy (at open circuit potential, counter electrode - Pt/Pt- black, AC frequency range 10^{-1} – 10^6 Hz, Solartron SI 1260A impedance and amplitude-phase analyzer, ZPlot and ZView2 software; "Solartron Analytical", UK).

Results and discussion

1. Morphology of oxide coatings on steel

The chemical composition of the gels and the conditions of their production affect on the morphology of the resulting coatings. By Fig. 3, SEM images of bilayer aluminium-oxide and silicon-oxide coatings compared to the surface of an uncoated heat-treated steel sample. By Fig. 3, Al_2O_3 layers are continuous, without cracks and large pores (see Fig. 3 *a, b*), but their morphology depends on the conditions under which the boehmite gel is obtained. The silicon oxide coating differs. It is homogeneous in structure, but large cracks form on it during drying and annealing, making the surface of the coated metal accessible to components of the corrosive environment. Even the application of a second coat does not help to improve cohesion (see Fig. 3, *c*).



There are single and bilayer Al_2O_3 - SiO_2 coatings obtained with different ratios of alumina gel to siliceous gel at Fig. 4. Obviously, such films have a large number of cracks that compromise the continuity of the coating. SiO_2 gel component gives these to the coatings. It is agree with the references [15, 16]. There is a large shrinkage of silicon oxide films during drying and annealing, accompanied by layer cracking.

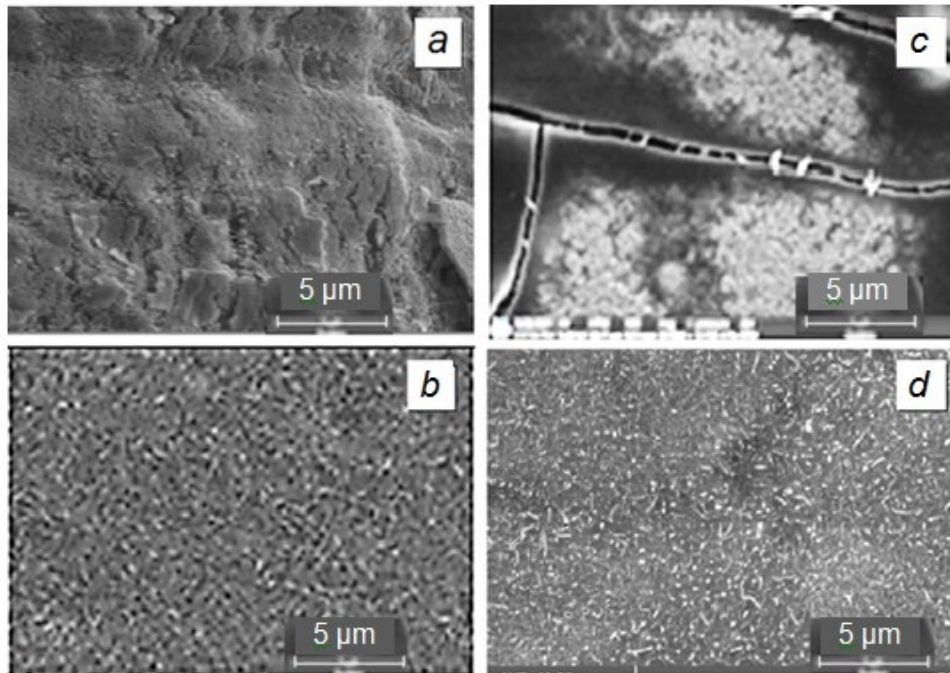


Fig. 3. SEM images of bi-coated steel samples: *a* - Al_2O_3 (gel with pH = 5); *b* - Al_2O_3 (gel with pH = 9.5); *c* - SiO_2 (gel with pH = 9.5); *d* - uncoated sample annealed at 500 °C in air

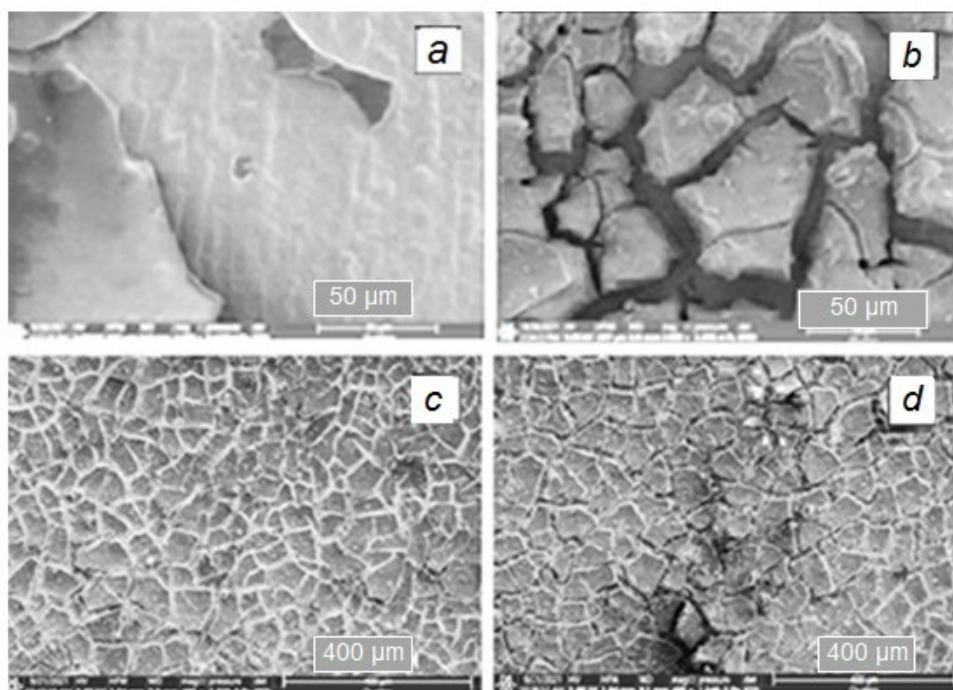


Fig. 4. SEM images of single layer (*a*, *b*) and double layer (*c*, *d*) coatings obtained from Al_2O_3 - SiO_2 gel at component ratios: 4:1 (*a*, *c*) and 1:4 (*b*, *d*)



2. Assessment of coating quality based on corrosion diagrams

There are corrosion diagrams of uncoated and coated steel samples in a naturally aerated 3.5% sodium chloride solution at Fig. 5. The values of steady-state potentials (E_{st}) of the investigated samples with coatings obtained from alkaline gels (see Fig. 5, *b* (curve 1), *c*, *d*), are close in their values to the E_{st} of uncoated steel (see Fig. 5, *a*). The coatings are defective to varying degrees on these samples. The sample with an Al_2O_3 layer obtained from a gel with acid peptization of the beohmite dispersion (see Fig. 5, *b*, curve 2), the shift of the stationary potential of the sample exceeds 0.7 V in the positive direction (compared to E_{st} of the original sample). This characterises the formed Al_2O_3 layer as an effective (defect-free) physical barrier preventing metal contact with the corrosive environment.

The corrosion of uncoated steel occurs at a cathodically controlled rate - limited by the rate of dissolved oxygen (cathodic depolariser) supplied to the corroding metal surface. The coatings change the nature of the anodic and cathodic branches of the corrosion diagram, and the corrosion process can proceed with both cathodic and anodic rate control. The calculation of the corrosion current density ($\log j_{cor}$) showed the only single-component Al_2O_3 films and two-component films with high aluminium oxide content have more or less well expressed protective properties towards the base. The j_{cor} values $\mu A/cm^2$: 35.5 (uncoated), 11.2 (Al_2O_3 , alkaline gel), 0.11 (Al_2O_3 , acidic gel) and 28.2 (Al_2O_3 - SiO_2 , 4:1).

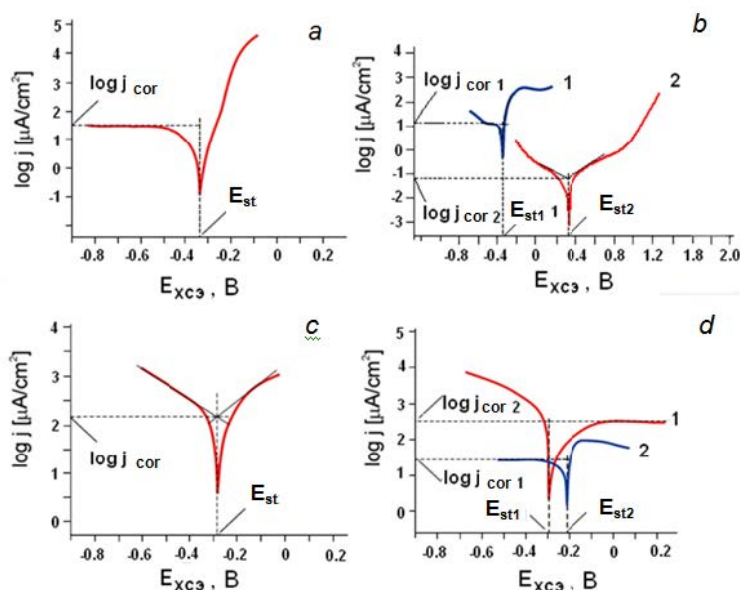


Fig. 5. Corrosion diagrams of 08kn steel samples: *a* - in the initial state ($E_{st} = -335$ mV) and with bilayer coatings: *b* - with oxide-aluminium coating obtained from gels with alkaline (curve 1, $E_{st} = -350$ mV) and acid (curve 2, $E_{st} = 410$ mV) peptization; *c* - with oxide-silicon coating obtained from gel with alkaline peptization ($E_{st} = -280$ mV); *d* - with two-component Al_2O_3 - SiO_2 coating obtained from mixture of gels with alkaline peptization at component ratio 1: 4 (curve 1, $E_{st} = -295$ mV) and 4:1 (curve 2, $E_{st} = -215$ mV). Potential sweep speed 1 mV/s. Temperature (23 ± 1) °C

3. Assessment of coating quality based on electrochemical impedance spectroscopy data

We study the corrosion kinetics of uncoated and coated steel samples by electrochemical impedance spectroscopy (EIS) in a naturally aerated 3.5% sodium chloride solution at an open



circuit potential. Fig. 6 shows the Bode diagrams (impedance modulus $|Z|$ and phase angle θ as a function of alternating current frequency) for the bilayer-coated samples, showing less corrosion current density in compare with the control sample. The best parameters (highest $|Z|$ and θ) show the oxide-aluminium-coated samples from the acidic gel (curves 2) and the two-component Al_2O_3 - SiO_2 -coatings.

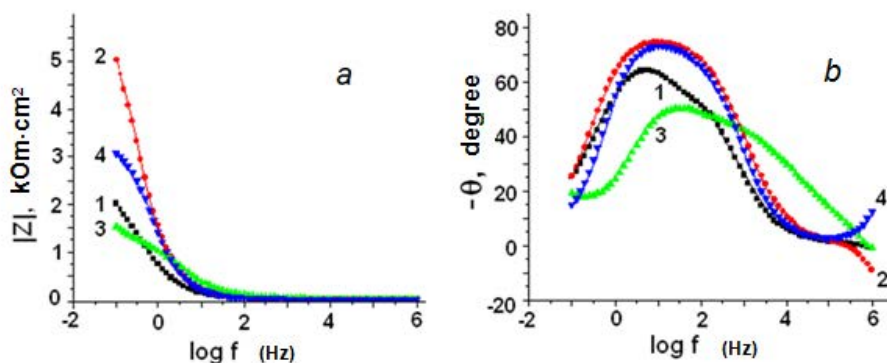


Fig. 6. Dependences of impedance modulus (a) and phase angle (b) on alternating current frequency for steel samples: 1 - uncoated; 2 - with bilayer Al_2O_3 coating (from gel with pH = 5); 3 - with bilayer Al_2O_3 coating (from gel with pH = 9); 4 - with bilayer two-component Al_2O_3 - SiO_2 coating (4:1 component ratio). Impedance parameters measured after 0.5 h of sample immersion in 3.5% NaCl, temperature $(23 \pm 1)^\circ\text{C}$

The metal-oxide-solution system was modelled by electric circuit analogy (ECA) (see Fig. 7). For this ECA R_{el} is the electrolyte resistance between the electrode under investigation and the auxiliary electrode; R_p is the resistive component of the coating; CPE is the constant phase element (non-ideal coating capacitance index), Z_{CPE} impedance can be represented by the expression [12, 19]

$$Z_{CPE} = \frac{1}{Q(j\omega)^n},$$

where Q is the constant of the CPE element ($\text{F cm}^{-2}\text{-s}^{-(1-n)}$); ω - circular frequency, $\omega = 2\pi f$ (rad s^{-1}); $j^2 = -1$ and n is the degree ratio of the CPE element (indicates the angle of depression, which characterises the deformation of the capacitive loop in the Nyquist diagram). CPE can be defined as capacitance when $n = 1$ at resistance $n = 0$ and as Warburg resistance at $n = 0.5$.



Fig. 7. ECA for the interpretation of electrochemical impedance spectroscopy data of barrier-coated metal

We calculated the ECA values for coated steel depending on the contact time of the samples with the corrosive medium (see Table 1). The increase of Q values is characterised for all the coatings. It depends on the increase of coating capacity due to the penetration of the solution into the pores and along with the increase of oxide layer area contact with the solution. It also leads to the decrease of R_p and n values.

The initial values of CPE parameter (Q and n) of Al_2O_3 layers obtained from gel with pH = 5 and the two-component Al_2O_3 - SiO_2 have comparable values. The rate of decrease of n



in both cases is 0.026 h^{-1} ($R^2 = -0.99$). But the rate of increase of parameter Q and decrease of R_p of one-component coating is almost two times higher than the two-component one (Fig. 8). Sufficiently high values of the parameter n indicate satisfactory quality of the formed layer. But they cannot be classified as purely capacitive due to the presence of pores gradually brought into contact with the electrolyte.

The Al_2O_3 coating obtained from a gel with $\text{pH} = 9$ fails the corrosion test due to the significantly higher defectiveness and permeability of the coating. It correlates with the data obtained by other methods.

Table 1. ECA values for coated samples in contact with 3.5% sodium chloride solution

Coating	Time, hours	ECA parameters		
		CPE		$R_p, \text{OM cm}^{-2}$
		$Q, \mu\text{F cm}^{-2} \text{c}^{-(1-n)}$	n	
Al_2O_3 – obtained from gel $\text{pH} = 5$	0.5	132.6	0.84	6.57
	1.0	149.3	0.84	4.76
	1.5	174.9	0.82	3.86
	2.0	211.4	0.81	3.33
	2.5	253.3	0.79	2.71
	3.0	274.3	0.78	2.55
	3.5	299.1	0.77	2.43
Al_2O_3 – obtained from gel $\text{pH} = 9$	0.5	197.8	0.59	1.85
	1.0	297.6	0.55	1.71
	1.5	381.5	0.53	1.68
	2.0	566.2	0.49	1.53
	3.0	Sharp increase		Sharp decrease
$\text{Al}_2\text{O}_3 - \text{SiO}_2$	0.5	119.7	0.86	4.02
	1.0	129.5	0.85	3.49
	1.5	134.8	0.85	3.15
	2.0	144.7	0.83	2.78
	3.0	193.2	0.80	1.83
	4.0	242.4	0.77	1.61

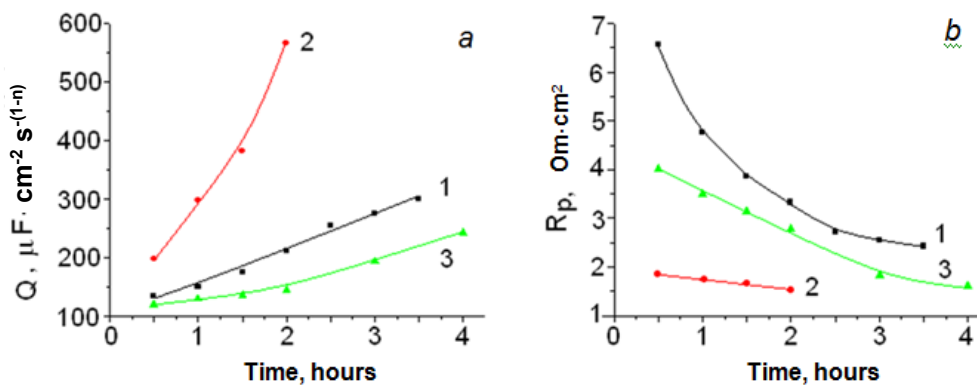


Fig. 8. ECA parameters Q (a) and R_p (b) as a function of contact time with 3.5% NaCl solution at temperature $(23 \pm 1) \text{ }^\circ\text{C}$ of steel: 1 - with bilayer Al_2O_3 coating (gel with $\text{pH} = 5$); 2 - with bilayer Al_2O_3 coating (gel with $\text{pH} = 9$); 3 - with bilayer two-component $\text{Al}_2\text{O}_3 - \text{SiO}_2$ coating (4:1 component ratio)



Conclusions

This paper devoted to the effect of pH on the characteristics of aluminium- and silicon-containing sol-gel systems as well as on the properties of oxide coatings formed on low-alloyed 08kp steel from these colloids.

The gels obtained with acetic acid as a peptisator exhibit high corrosion activity then the gel layer is dried on the metal. For aluminogel we solved this problem earlier by drying the layer in ammonia vapour [13, 14]. But for siliceous gel this method is proved ineffective. The use of gels with peptisation of hydrated oxide particles using ammonia solution (pH = 9–11) prevents the development of corrosion on steel during coating application and drying. Meanwhile, alkaline peptisation produces larger particles of hydrated aluminium and silicon oxides.

The coatings formed from acidic and alkaline aluminogels, alkaline siliceous gel and their mixtures at various component ratios. Thus, the one-component SiO₂-coating and the presence of SiO₂ in two-component coatings leads to the formation of micro-cracks, which negatively effect on the anti-corrosion properties of the films.

Voltammetry and electrochemical impedance spectroscopy help to study the protective properties of coatings in 3.5% sodium chloride solution at (23±1) °C. We calculated corrosion current densities by corrosion diagrams and only single-component Al₂O₃-films and two-component films with high aluminium oxide content have protective effect. Electrochemical impedance spectroscopy data modeled the metal-film-electrolyte interface using an equivalent electrical circuit. The work contains the calculations of the values of the circuit parameters and their variation as a function of sample exposure time. The oxide-aluminium films made from aluminogel with pH = 5 and two-component Al₂O₃-SiO₂ films of 4:1 composition show the best results.

The study was under financial support of the Russian Foundation for Basic Research and the Ivanovo Region Administration as part of Scientific Project No. 18-43-370030_r_a.

References

1. Corrosion: Handbook / ed. by L.L. Schreyer. M.: Metallurgy, 1981. 632 p. (in Russian).
2. Bahuguna G., Kumar Mishra N., Chaudhary P., Kumar A., Singh R. Thin Film Coating through Sol-Gel Technique. *Research Journal of Chemical Sciences*. 2016. V. 6 (7). P. 65-72.
3. Durán A., Castro Y., Conde A., Damborenea J.J. Sol-Gel Protective Coatings for Metals. *Handbook of Sol-Gel Science and Technology. Sol-Gel Protective Coatings for Metals*. Berlin: Springer, 2018. P. 2369–2433. DOI: 10.1007/978-3-319-32101-1_70.
4. Zheludkevich M.L., Miranda Salvado I., Ferreira M.G.S. Sol-gel coatings for corrosion protection of metals. *Journal of Materials Chemistry*. 2005. V. 15. P. 5099-5111. DOI: 10.1039/b419153f.
5. Wang D., Bierwagen G.P. Sol-gel coatings on metals for corrosion protection. *Progress in Organic Coatings*. 2009. V. 64. P. 327-338. DOI: 10.1016/j.porgcoat.2008.08.010.
6. Yoldas B.E. Alumina sol preparation from alkoxides. *Ceramic Society Bull.* 1975. V. 54. P. 289-290.
7. Yoldas B.E. US Patent N 3,944,658. 1976.
8. Maksimov A.I., Moshnikov V.A., Tairov Yu.M., Shilova O.A. Fundamentals of sol-gel technology of nanocomposites. Saint-Petersburg: OOO "Technomedia", Elmore Publisher, 2008. 255 p. (in Russian).
9. Doodman P., Faghihi-Sani M.A., Barati N., Afshar A. Alumina nanostructured coating for corrosion protection of 316L stainless steel. *International Journal Nano Dimens.* 2014. V. 5(1). P. 27-33. DOI: 10.7508/ijnd.2014.01.004.



10. **Tiwari S.K., Sahu R.K., Pramanick A.K., Singh R.** Development of conversion coating on mild steel prior to sol gel nanostructured Al_2O_3 coating for enhancement of corrosion resistance. *Surface and Coatings Technology*. 2011. V. 205. P. 4960-4967. DOI: 10.1016/j.surfcoat.2011.04.087.
11. **Alan G., Sajin G., Tinu T., Vibhath K., Sreejith M.** Corrosion Behavior of Sol-Gel Derived Nano-Alumina Film. *International Journal of Scientific & Engineering Research*. 2016. V. 7. N 3. P. 130-139.
12. **Ruhi G., Modi O.P., Singh I.B.** Corrosion behaviour of nano structured sol-gel alumina coated 9Cr-1Mo ferritic steel in chloride bearing environments. *Surface and Coatings Technology*. 2009. V. 204. P. 359-365. DOI: 10.1016/j.surfcoat.2009.07.044.
13. **Grishina E.P., Kudryakova N.O., Ramenskaya L.M.** Characterization of the properties of thin Al_2O_3 films formed on structural steel by the sol-gel method. *Condensed Matter and Interphases*. 2020. V. 22. N 1. P. 39-47. DOI: 10.17308/kcmf.2020.22/2527.
14. **Grishina E.P., Kudryakova N.O., Ramenskaya L.M.** Application of sol-gel method for the formation of alumina coating on low-alloyed steel. *Gal'vanotekhnika i obrabotka poverhnosti*. 2019. T. 27. № 2. P. 59-68. DOI: 10.47188/0869-5326_2019_27_2_59 (in Russian).
15. **Mora L.V., Naik S., Paul S., Dawson R., Neville A., Barker R.** Influence of silica nanoparticles on corrosion resistance of sol-gel based coatings on mild steel. *Surface and Coatings Technology*. 2017. V. 324. P. 368-375. DOI: 10.1016/j.surfcoat.2017.05.063.
16. **Mora L.V., Taylor A., Paul S., Dawson R., Wang C., Taleb W., Owen J., Neville A., Barker R.** Impact of silica nanoparticles on the morphology and mechanical properties of sol-gel derived coatings. *Surface and Coatings Technology*. 2018. V. 342. P. 48-56. DOI: 10.1016/j.surfcoat.2018.02.080.
17. **Gasiorek J., Szczurek A., Babiarczuk B., Kaleta J., Jones W., Krzak J.** Functionalizable Sol-Gel Silica Coatings for Corrosion Mitigation. *Materials*. 2018. V. 11. P. 197. DOI:10.3390/ma11020197.
18. **Phanasgaonkar A., Raja V.S.** Influence of curing temperature, silica nanoparticles and cerium on surface morphology and corrosion behaviour of hybrid silane coatings on mild steel. *Surface and Coatings Technology*. 2009. V. 203. P. 2260-2271. DOI: 10.1016/j.surfcoat.2009.02.020.
19. **Singh I.B., Modi O.P., Ruhi G.** Development of sol-gel alumina coating on 9Cr-1Mo ferritic steel and their oxidation behavior at high temperature. *Journal Sol-Gel Science and Technology*. 2015. V. 74. P. 685-691. DOI:10.1007/s10971-015-3649-9.

Received 01.12.2021

Accepted 09.12.2021